Transmission and Attenuation of Vector Modes in Uniformly Bent Circular Hollow Waveguides for the Infrared

Shin-ichi Abe and Mitsunobu Miyagi, *Senior Member, IEEE*

***Abstract*—Electric field distributions and attenuation constants of the eigenmodes in uniformly bent circular hollow waveguides have been evaluated based on a vector wave equation deduced from Maxwell's equations. A diagram representation of the parameter describing mode properties has been newly introduced. It is numerically shown that vector modes gradually approach linearly polarized modes when the bending radius becomes small. A relation between attenuation constants in sharply bent circular and slab hollow waveguides is also discussed where the electric fields concentrate near the outer edge of the core.**

I. Introduction

CIRCULAR hollow waveguides have been studied for delivering infrared high power [1], [2]. In practical uses, these waveguides are often bent, hence, electric and magnetic field distributions are deformed and transmission losses increase. Therefore, it is important to evaluate field distributions and losses in bent circular hollow waveguides precisely.

In uniformly bent waveguides, a vector analysis was developed by using perturbation theory [3]. Although the field deformations and polarization changes in waveguides were analyzed in detail, the analysis itself is limited to the waveguides with a large bending radius. Marhic *et al.* analyzed a whispering-gallery waveguide where the bending is an essential issue [4]. They employed a boundary condition used in the microwave regions which is not necessarily applied to infrared waveguides. A ray analysis was also made by Croitoru *et al.* which is substantially based on an approximate scalar equation [5].

In a previous paper [6], we analyzed the lowest eigenmode in bent circular hollow waveguides based on the scalar equation. The field distributions were first evaluated by assuming that they vanish at the core-cladding boundary and attenuation constants were then evaluated by using an integral expression which includes the approximate fields.

In straight circular hollow waveguides, there exist TE_{0m}, TM_{0m}, HE_{nm} and EH_{nm} modes ($n = 1, 2, \cdots, m = 1, 2, \cdots$) which are not linearly polarized except for the HE_{1m} modes. When waveguides are bent, many modes are excited. Therefore, it is important to explore the properties of vector modes in bent circular waveguides.

In this paper, we treat several lower-order TE_{01}, TM_{01}, and HE_{21} modes. To solve a vector wave equation, we express a solution of the equation by a linear combination of linearly polarized modes derived from a corresponding scalar equation. The mode structures and attenuation constants of the TE_{01}, TM_{01}, and HE_{21} modes in bent circular hollow waveguides have been clarified. Throughout the paper, the wavelength is assumed to be 10.6 μm of the CO_2 laser.

II. Formulation

We analyze low-loss circular hollow waveguides for infrared laser beams. We assume that the core radius is much larger than the wavelength of transmitted light and that the normalized surface impedance z_{TE} and admittance y_{TM} [7] defined at the core-cladding boundary are sufficiently small compared with the impedance and admittance in the core region. We are interested in the waveguide whose bending radius is larger than several tens times of the core radius.

Using the toroidal coordinate system (r, θ, z) as shown in Fig. 1, the transverse electric field $\mathbf{E}_t$ with the axial (z-direction) phase constant β, satisfies

$$\frac{\partial^2 \mathbf{E}_t}{\partial r^2} + \frac{1}{r}\frac{\partial \mathbf{E}_t}{\partial r} + \frac{1}{r^2}\frac{\partial^2 \mathbf{E}_t}{\partial \theta^2} + \left[n_0^2 k_0^2 \left(1 + 2\frac{r}{R}\cos\theta\right) - \beta^2\right]\mathbf{E}_t = 0, \quad (1)$$

in the core region [6], where k_0 is the wavenumber in free space. We solve (1) with the boundary conditions at $r = T$:

$$\frac{E_\theta}{H_z} = \frac{\omega\mu_0}{n_0 k_0} z_{TE}, \quad (2a)$$

$$\frac{H_\theta}{E_z} = -\frac{n_0 k_0}{\omega\mu_0} y_{TM}. \quad (2b)$$

Manuscript received July 30, 1991; revised December 16, 1991. This work was supported by a Scientific Research Grant-in-Aid (0240236) from the Ministry of Education, Science, and Culture of Japan.

The authors are with the Department of Electrical Communications, Faculty of Engineering, Tohoku University, Sendai, 980, Japan.

IEEE Log Number 9106771.

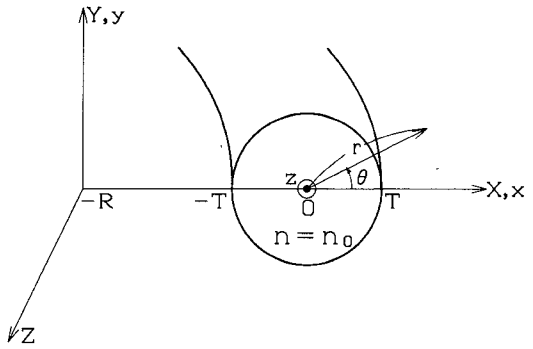

Fig. 1. Toroidal coordinate system for bent circular hollow waveguides.

First, we consider the transverse electric field $\tilde{\mathbf{E}}_t$ which satisfies the following boundary conditions at $r = T$:

$$z_{TE} = y_{TM} = 0. \tag{3}$$

i.e.,

$$\tilde{\mathbf{E}}_t = 0. \tag{4}$$

By letting the axial phase constant be $\tilde{\beta}$ which corresponds to $\tilde{\mathbf{E}}_t$, $\tilde{\mathbf{E}}_t$ satisfies

$$\frac{\partial^2 \tilde{\mathbf{E}}_t}{\partial r^2} + \frac{1}{r}\frac{\partial \tilde{\mathbf{E}}_t}{\partial r} + \frac{1}{r^2}\frac{\partial^2 \tilde{\mathbf{E}}_t}{\partial \theta^2} + \left[n_0^2 k_0^2 \left(1 + 2\frac{r}{R}\cos\theta\right) - \tilde{\beta}^2\right]\tilde{\mathbf{E}}_t = 0, \tag{5}$$

in the core region.

Modes which satisfy (4) and (5) are characterized by linearly polarized modes, which are constructed from even symmetrical $\tilde{E}_e$ and odd symmetrical $\tilde{E}_o$ scalar modes with respect to θ.

We now expand $\tilde{E}_e$ and $\tilde{E}_o$ by using the Fourier–Bessel series as follows:

$$\tilde{E}_e(r, \theta) = \sum_{\nu=0}^{\infty}\sum_{p=1}^{\infty} A_{\nu p}^e J_\nu\left(\sigma_{\nu p}\frac{r}{T}\right)\cos(\nu\theta), \tag{6a}$$

$$\tilde{E}_o(r, \theta) = \sum_{\nu=1}^{\infty}\sum_{p=1}^{\infty} A_{\nu p}^o J_\nu\left(\sigma_{\nu p}\frac{r}{T}\right)\sin(\nu\theta), \tag{6b}$$

where $\sigma_{\nu p}$ is the pth zero of $J_\nu(x)$. The expansion coefficients $A_{\nu p}^e$, $A_{\nu p}^o$ and the axial phase constants $\tilde{\beta}_e$ and $\tilde{\beta}_o$, which correspond to even and odd modes respectively, are determined by substituting (6a) and (6b) to (5) and using the orthogonal relations by Bessel or trigonometric functions [6]. It should be noted that $A_{\nu p}^e$, $A_{\nu p}^o$, $\tilde{\beta}_e$, and $\tilde{\beta}_o$ are a function only of bending parameter b [6] defined by

$$b = \frac{n_0^2 k_0^2 T^3}{R}. \tag{7}$$

We now describe how to derive the vector field $\mathbf{E}_t$ satisfying the boundary conditions (2a) and (2b) by using fields $\tilde{\mathbf{E}}_t$ satisfying (3). The method employed here is similar to that developed by Snyder *et al.* [8] who derived vector modes in weakly guiding fibers fibers from the LP modes in a scalar wave equation. The essential difference between weakly guiding fibers and present hollow waveguides is that the cladding indices are completely different in the two cases, i.e., in infrared hollow waveguides the (complex) refractive index is much higher than that of the hollow core. However, both waveguides have a very similar property in that modes whose axial phase constants are around $n_0 k_0$ are nearly degenerate. Therefore, it is easily understood that we are able to construct vector modes in even bent hollow waveguides by combining linearly polarized modes in the scalar wave equation.

Applying Green's theorem to the surface integral of $\tilde{\mathbf{E}}_t \cdot$ [(1)] $-$ $\mathbf{E}_t \cdot$ [(5)] in the core region, we obtain

$$(\beta^2 - \tilde{\beta}^2)\int\int_S \mathbf{E}_t \cdot \tilde{\mathbf{E}}_t \, dS + \oint_C \mathbf{E}_t \cdot \frac{\partial \tilde{\mathbf{E}}_t}{\partial r}\,\mathrm{dc} = 0, \tag{8}$$

where S is a cross sectional area of circular core and the C is the periphery defined by $r = T$.

Let us express the transverse electric field $\mathbf{E}_t$ of vector modes by linear combinations of the linearly polarized modes $\hat{x}\tilde{E}_x$ and $\hat{y}\tilde{E}_y$ as

$$\mathbf{E}_t(r, \theta) = \hat{x}P_x\tilde{E}_x + \hat{y}P_y\tilde{E}_y, \tag{9}$$

where $\hat{x}$ and $\hat{y}$ are unit vectors in the x and y directions, respectively, and P_x and P_y are arbitrary constants to be determined. As is seen from the subsequent formulation, there are only combinations of $\tilde{E}_x$ and $\tilde{E}_y$ which are even and odd, respectively, with respect to θ, or vice versa. Since a number of even or odd linearly polarized modes exist, the combinations of linearly polarized modes should be considered. However, for the waveguides which will be treated in Section III, only the combination of an even linearly polarized mode and an odd linearly polarized mode with the same mode number is important. Therefore, we consider the linear combinations of only two linearly polarized modes described by (6a) and (6b) in the subsequent formulation.

We first consider the case that $\tilde{E}_x = \tilde{E}_e$ and $\tilde{E}_y = \tilde{E}_o$ in (9). Since $\mathbf{E}_t$ should not vanish at $r = T$ in the vector modes, the transverse electric field at $r = T$ can be represented as follows [see Appendix]:

$$\mathbf{E}_t = \frac{j}{n_0 k_0}\left[\hat{x}\left\{P_x\frac{\partial \tilde{E}_e}{\partial r}(z_{TE}\sin^2\theta + y_{TM}\cos^2\theta) + P_y\frac{\partial \tilde{E}_o}{\partial r}(y_{TM} - z_{TE})\sin\theta\cos\theta\right\} + \hat{y}\left\{P_x\frac{\partial \tilde{E}_e}{\partial r}(y_{TM} - z_{TE})\sin\theta\cos\theta + P_y\frac{\partial \tilde{E}_o}{\partial r}(z_{TE}\cos^2\theta + y_{TM}\sin^2\theta)\right\}\right]. \tag{10}$$

We now substitute (9) and (10) into (8). By putting $\tilde{\mathbf{E}}_t = \hat{x}\tilde{E}_e$, we obtain

$$P_x(\beta^2 - \tilde{\beta}_e^2) + \frac{j}{n_0 k_0}\left[P_x\left\{z_{TE}\oint_C\left(\frac{\partial \tilde{E}_e}{\partial r}\sin\theta\right)^2 dc + y_{TM}\oint_C\left(\frac{\partial \tilde{E}_e}{\partial r}\cos\theta\right)^2 dc\right\} + P_y(y_{TM} - z_{TE})\oint_C \frac{\partial \tilde{E}_e}{\partial r}\frac{\partial \tilde{E}_o}{\partial r}\sin\theta\cos\theta\, dc\right] = 0, \tag{11a}$$

similarly, by putting $\tilde{\mathbf{E}}_t = \hat{y}\tilde{E}_o$ in (8), we obtain

$$P_y(\beta^2 - \tilde{\beta}_o^2) + \frac{j}{n_0 k_0}\left[P_y\left\{z_{TE}\oint_C\left(\frac{\partial \tilde{E}_o}{\partial r}\cos\theta\right)^2 dc + y_{TM}\oint_C\left(\frac{\partial \tilde{E}_o}{\partial r}\sin\theta\right)^2 dc\right\} + P_x(y_{TM} - z_{TE})\oint_C \frac{\partial \tilde{E}_e}{\partial r}\frac{\partial \tilde{E}_o}{\partial r}\sin\theta\cos\theta\, dc\right] = 0, \tag{11b}$$

where $\tilde{E}_e$ and $\tilde{E}_o$ are normalized such that the integral of $\tilde{E}_e^2$ or $\tilde{E}_o^2$ over the cross section is unity. Equations (11a) and (11b) are simultaneous equations which determine P_x, P_y, and β.

By introducing the normalized transverse phase constant U of vector modes defined by

$$U = T(n_0^2 k_0^2 - \beta^2)^{1/2}, \tag{12}$$

(11a) and (11b) are transformed to the matrix equation as

$$\mathbf{M}\begin{pmatrix} P_x \\ P_y \end{pmatrix} = U^2\begin{pmatrix} P_x \\ P_y \end{pmatrix}, \tag{13}$$

where elements of $\mathbf{M}$ are represented as follows:

$$M_{11} = \tilde{U}_e^2 + \frac{j}{n_0 k_0 T}\left[z_{TE}T^3\oint_C\left(\frac{\partial \tilde{E}_e}{\partial r}\sin\theta\right)^2 dc + y_{TM}T^3\oint_C\left(\frac{\partial \tilde{E}_e}{\partial r}\cos\theta\right)^2 dc\right], \tag{14a}$$

$$M_{12} = M_{21} = \frac{j}{n_0 k_0 T}(y_{TM} - z_{TE})\,T^3\oint_C \frac{\partial \tilde{E}_e}{\partial r}\frac{\partial \tilde{E}_o}{\partial r}\cdot \sin\theta\cos\theta\, dc, \tag{14b}$$

$$M_{22} = \tilde{U}_o^2 + \frac{j}{n_0 k_0 T}\left[z_{TE}T^3\oint_C\left(\frac{\partial \tilde{E}_o}{\partial r}\cos\theta\right)^2 dc + y_{TM}T^3\oint_C\left(\frac{\partial \tilde{E}_o}{\partial r}\sin\theta\right)^2 dc\right], \tag{14c}$$

$\tilde{U}_e$ and $\tilde{U}_o$ are defined by (12) where β is replaced by the axial phase constants $\tilde{\beta}_e$ and $\tilde{\beta}_o$ of even and odd symmetrical linearly polarized modes, respectively. As is seen from (14a)–(14c), vector modes are completely characterized by the bending parameter b and the waveguide parameters of $z_{TE}/n_0 k_0 T$ and $y_{TM}/n_0 k_0 T$. Two independent vector modes are derived from (13). When only the term with $\nu = 1$ and $p = m$ remains in (6a) and (6b) in straight waveguides, bending characteristics of the TM_{0m} and HE_{2m}^e modes [8] are derived.

Similarly, considering the case that $\tilde{E}_x = \tilde{E}_o$ and $\tilde{E}_y = \tilde{E}_e$ in (9), two other independent vector modes are derived. For the modes where the term with $\nu = 1$ and $p = m$ is dominant in (6a) and (6b), bending characteristics of the HE_{2m}^o [8] and TE_{0m} modes in straight waveguides are derived.

III. Eigenmodes in Bent Circular Hollow Waveguides

In this section, we numerically evaluate field distributions and attenuation constants of the TE_{01}, TM_{01}, HE_{21}^e, and HE_{21}^o modes in bent circular hollow waveguides as vector modes. We clarify mode properties of the zinc-selenide coated silver hollow waveguide which is designed so as the transmission loss becomes minimum, silica hollow, and sapphire hollow waveguides. The parameters which are used in the numerical analysis of each waveguide are summarized in Table I.

A. Polarization Properties of Eigenmodes

In order to see mode property changes due to bend, we newly introduce a parameter Q defined by

$$Q = (P_y/P_x)/(1 + |P_y/P_x|^2)^{1/2}, \tag{15}$$

which indicates a relative magnitude between E_x and E_y.

Fig. 2 shows the parameter Q of the above modes in silica hollow, sapphire hollow, and zinc-selenide coated silver hollow waveguides in the complex Q-plane. In straight waveguides ($b = 0$), the parameter Q of the TM_{01} and HE_{21}^o modes is equal to $1/\sqrt{2}$ and that of HE_{21}^e and TE_{01} modes is $-1/\sqrt{2}$. That the value of Q is complex means that the local electric fields are elliptically polarized with different aspect ratios. When the parameter b becomes large, the parameter Q in all waveguides approaches 0 in the TM_{01} and HE_{21}^e modes, and $|Q|$ approaches unity in the HE_{21}^e and TE_{01} modes, which means that the TM_{01} and TE_{01} modes change to linearly polarized (LP) mode whose polarization direction is in the x axis, and the HE_{21}^e and HE_{21}^o modes change to the LP mode whose polarization direction is in the y axis.

As described in Section III-B, the electric field distribution of each mode tends to concentrate near the outer edge of the waveguide around $\theta = 0$. This indicates that the polarization of each mode is quite influenced by the boundary conditions at $\theta = 0$. As the round structure therefore quite resemble to the slab waveguide, there exist independent linearly polarized modes whose polarizations are perpendicular and parallel to the bending plane.

Loci of Q show very different behaviors between the silica hollow waveguide and others. Loci in the silica hollow waveguide tend to vary away from the real axis, while

TABLE I
Z_{TE}/n_0k_0T and y_{TM}/n_0k_0T IN SILICA, SAPPHIRE, AND ZINC-SELENIDE COATED SILVER HOLLOW WAVEGUIDES, WHERE $\lambda = 10.6\ \mu m$, $n_0 = 1$, and $T = 0.5$ mm

Cladding Material	z_{TE}/n_0k_0T	y_{TM}/n_0k_0T
Silica	$1.7 \times 10^{-3} + j9.7 \times 10^{-5}$	$8.4 \times 10^{-3} - j2.9 \times 10^{-4}$
Sapphire	$1.6 \times 10^{-4} + j4.5 \times 10^{-3}$	$2.6 \times 10^{-4} + j2.0 \times 10^{-3}$
ZnSe-coated-Ag	$2.7 \times 10^{-5} + j2.4 \times 10^{-3}$	$7.6 \times 10^{-5} - j5.6 \times 10^{-3}$

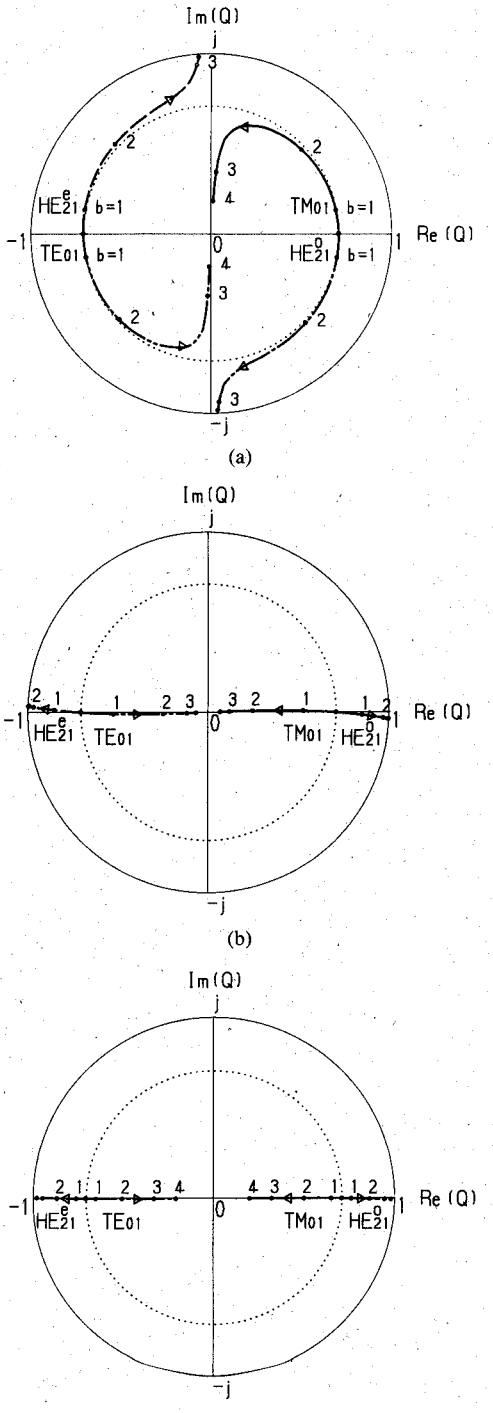

Fig. 2. Loci of Q in silica hollow (a), sapphire hollow (b), and zinc-selenide coated silver hollow waveguides (c), in the complex plane. The numbers near curves indicate values of b. A radius of the circle drawn by a dashed line is $1/\sqrt{2}$.

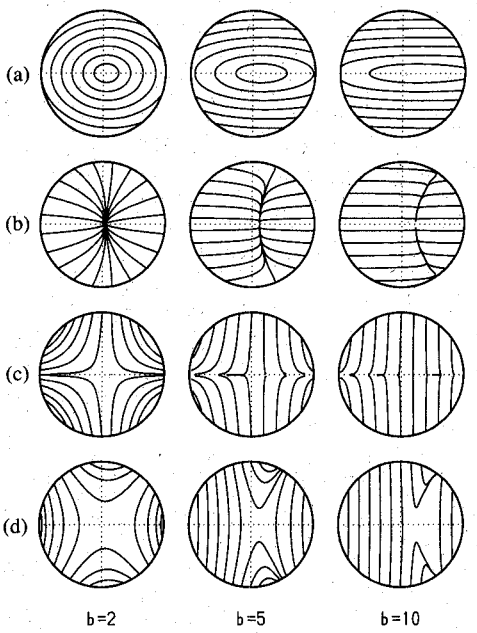

Fig. 3. Change of electric field lines of the TE_{01} (a), TM_{01} (b), HE^e_{21} (c), and HE^o_{21} modes (d), due to bent.

loci in others vary almost along the real axis. This difference comes from waveguide parameters as shown in Table I: in the silica hollow waveguide, we have

$$\text{Re}\,(z_{TE}/n_0k_0T) \gg \text{Im}\,(z_{TE}/n_0k_0T), \quad (16a)$$

$$\text{Re}\,(y_{TM}/n_0k_0T) \gg \text{Im}\,(y_{TM}/n_0k_0T), \quad (16b)$$

and in others, we have

$$\text{Re}\,(z_{TE}/n_0k_0T) \ll \text{Im}\,(z_{TE}/n_0k_0T), \quad (16c)$$

$$\text{Re}\,(y_{TM}/n_0k_0T) \ll \text{Im}\,(y_{TM}/n_0k_0T). \quad (16d)$$

Fig. 3(a)–(d) shows changes of electric field lines of the TE_{01}, TM_{01}, HE^e_{21}, and HE^o_{21} modes due to bends in the zinc-selenide coated silver hollow waveguides where Q is approximately real. One can see how the vector modes approach LP modes whose polarization direction is in the x or y direction.

B. Electric Field Intensity Distributions of Linearly Polarized Modes

As mentioned in Section III-A, eigenmodes in bent circular hollow waveguides approach linearly polarized modes when the parameter b increases, i.e., the curvature increases. Therefore, we calculate intensity distributions

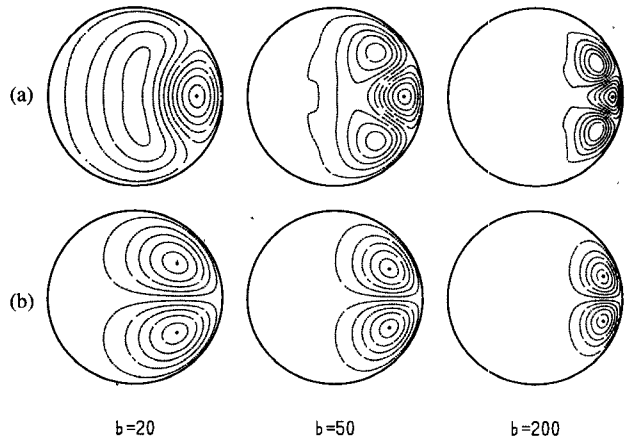

Fig. 4. Equi-field amplitude lines of transverse electric field distributions of linearly polarized even mode (a) and odd mode (b). Equi-field lines indicate ±0.1, ±0.3, ±0.5, ±0.7 and ±0.9, where the maximum amplitude is normalized to unity.

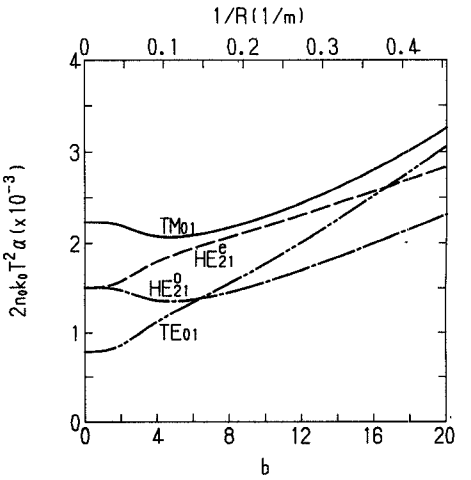

Fig. 5. Attenuation constants in the zinc-selenide coated silver hollow waveguide in the region $0 \leqq b \leqq 20$. The upper scale corresponds to the curvature for the same values of λ, n_0, and T in Table 1.

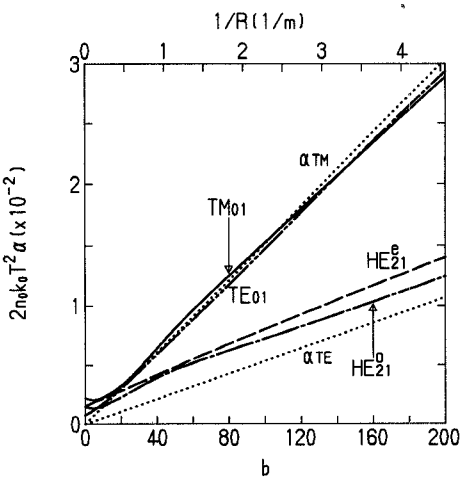

Fig. 6. Attenuation constants in the zinc-selenide coated silver hollow waveguide in the region $0 \leqq b \leqq 200$. The upper scale corresponds to the curvature for the same values of λ, n_0, and T in Table I.

of the even and odd LP_{11} modes whose nomenclature is given in a straight waveguide.

Fig. 4(a) and (b) shows equi-intensity lines of the even and odd symmetric LP_{11} modes for various curvatures. In the case of the odd symmetric LP_{11} mode (b), electric field distributions tend to concentrate near the outer edge with maintaining its field profile as curvature. On the other hand, a very different picture is found for the even symmetric mode (a) from that of the straight waveguide. There are three peaks near the outer edge of the waveguide perpendicular to the bending plane. As the waveguide is bent, inner and outer peaks of field distributions shift toward the outer edge and approach each other. The outer peak is larger than the inner peak. Then, the center of the inner peak may be canceled by the outer peak when the both peaks approach each other. This is why the inner peak is separated into two peaks.

C. Attenuation Constants of Eigenmodes

By approximating the real part of β by n_0k_0 in (12), the attenuation constant is represented by

$$2\alpha = \frac{\mathrm{Im}\,(U^2)}{n_0k_0T^2}. \tag{17}$$

Fig. 5 shows the attenuation constants in the zinc-selenide coated silver hollow waveguide in the region $0 \leqq b \leqq 20$. The magnitudes of the attenuation constants in gently bent waveguides ($b \leqq 2$) are TM_{01}, HE_{21}^e, HE_{21}^o, and TE_{01} modes, in order. However, as the curvature increases, the attenuation constant of the TE_{01} mode becomes larger than that of the HE_{21}^o mode. In the region, $b \geqq 18$, the magnitudes of attenuation constants are TM_{01}, TE_{01}, HE_{21}^e, and HE_{21}^o modes, in order. This is because modes change to the linearly polarized mode as the curvature increases.

Fig. 6 shows the attenuation constants in the zinc-selenide coated silver hollow waveguide in the region $0 \leqq b \leqq 200$. When the curvature is large, modes are classified into linearly polarized modes whose polarization direction is in the x or y direction. It should be noted that the difference of attenuation constants of the modes with same polarization is relatively small and also that attenuation constants of the two linearly polarized modes along the x direction are much larger than those of two modes along the y direction. This indicates that the main factor which determines the magnitudes of attenuation constants is the polarization direction.

In Fig. 6, α_{TE} and α_{TM} defined by

$$\alpha_{TE} = \frac{1}{R}\,\mathrm{Re}\,(z_{TE}), \tag{18a}$$

$$\alpha_{TM} = \frac{1}{R}\,\mathrm{Re}\,(y_{TM}), \tag{18b}$$

are also shown, which are attenuation constants of the TE and TM modes in sharply bent slab hollow waveguide [9]. Roughly speaking, the attenuation constants of the LP_{11} modes whose polarization direction is parallel to the

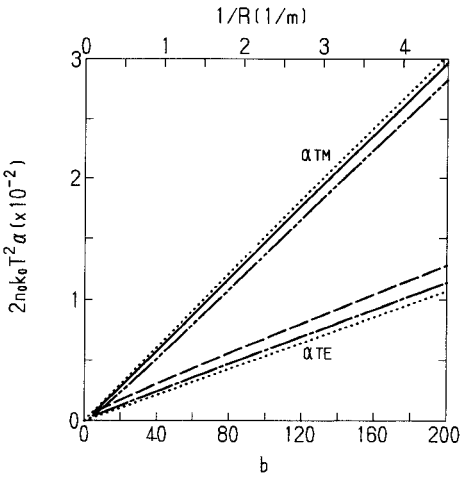

Fig. 7. Attenuation constants predicted by [10] in the zinc-selenide coated silver hollow waveguide. The modes shown in the figure are selected to correspond to the modes that we present. The upper scale corresponds to the curvature for the same values of λ, n_0, and T in Table I.

bending plane can be well estimated by the attenuation constant α_{TM}. However, this does not necessarily mean that the attenuation constant of the modes asymptotically approach to α_{TM} [10]. A relatively large difference is found between α_{TE} and those of LP_{11} modes whose polarization direction is perpendicular to the bending plane. This difference will be emphasized for the waveguides where the magnitudes of the surface impedance and admittance are quite different.

We finally compare our present results of Fig. 6 with previously published results. Fig. 7 shows attenuation constants predicted by [10] for the linearly polarized modes where α_{TE} and α_{TM} for the corresponding slab waveguide are also shown for comparison. Qualitatively similar results are obtained for the linearly polarized modes changing from TE_{01} and TM_{01} modes.

IV. Conclusion

Based on the vector wave equation, mode structures and transmission losses of the TE_{01}, TM_{01}, and HE_{21} modes in uniformly bent circular hollow waveguides have been evaluated. Electric field distributions and the normalized transverse phase constant of eigenmodes are determined by the bending parameter b and the waveguide parameters z_{TE}/n_0k_0T and y_{TM}/n_0k_0T. It is shown that the TE_{01} and TM_{01} modes approach the LP mode whose polarization direction is parallel to the bending plane and the HE_{21} modes to the LP mode whose polarization direction is perpendicular to the bending plane.

Appendix

In lower-order eigenmodes of low-loss circular hollow waveguides, E_r is represented by

$$E_r = -j\frac{1}{\omega\epsilon_0 n_0^2}\left(\frac{1}{r}\frac{\partial H_z}{\partial\theta} + j\beta H_\theta\right) \doteqdot \frac{\omega\mu_0}{n_0k_0}H_\theta. \tag{A1}$$

By using tangential electric and magnetic field components, the transverse electric field $\mathbf{E}_t$ is represented as

$$\begin{aligned}\mathbf{E}_t &= \hat{r}E_r + \hat{\theta}E_\theta \\ &\doteqdot \hat{r}\frac{\omega\mu_0}{n_0k_0}H_\theta + \hat{\theta}E_\theta \\ &= \hat{x}\left(\frac{\omega\mu_0}{n_0k_0}H_\theta\cos\theta - E_\theta\sin\theta\right) \\ &\quad + \hat{y}\left(\frac{\omega\mu_0}{n_0k_0}H_\theta\sin\theta + E_\theta\cos\theta\right).\end{aligned} \tag{A2}$$

At the core-cladding boundary, (A2) is expressed by using the boundary conditions (2a) and (2b) and axial electric and magnetic field components as follows:

$$\begin{aligned}\mathbf{E}_t &= \hat{x}\left(-\frac{\omega\mu_0}{n_0k_0}z_{TE}H_z\sin\theta - y_{TE}E_z\cos\theta\right) \\ &\quad + \hat{y}\left(\frac{\omega\mu_0}{n_0k_0}z_{TE}H_z\cos\theta - y_{TE}E_z\sin\theta\right).\end{aligned} \tag{A3}$$

By considering that the transverse electric and magnetic field components at $r = T$ are sufficiently small, the axial electric and magnetic field components are represented as

$$\begin{aligned}E_z &= -j\frac{1}{\omega\epsilon_0 n_0^2}\left(\frac{\partial H_\theta}{\partial r} - \frac{1}{r}\frac{\partial H_r}{\partial\theta}\right) \\ &\doteqdot -j\frac{1}{\omega\epsilon_0 n_0^2}\frac{n_0k_0}{\omega\mu_0}\frac{\partial E_r}{\partial r} \\ &= -j\frac{1}{n_0k_0}\left(\frac{\partial E_x}{\partial r}\cos\theta + \frac{\partial E_y}{\partial r}\sin\theta\right),\end{aligned} \tag{A4}$$

$$H_z = -j\frac{1}{n_0k_0}\left(\frac{\partial E_x}{\partial r}\sin\theta - \frac{\partial E_y}{\partial r}\cos\theta\right). \tag{A5}$$

By substituting (A4) and (A5) into (A3), we obtain

$$\begin{aligned}\mathbf{E}_t = j\frac{1}{n_0k_0}\Bigg[&\hat{x}\left\{\frac{\partial E_x}{\partial r}(z_{TE}\sin^2\theta + y_{TM}\cos^2\theta)\right. \\ &\left. + \frac{\partial E_y}{\partial r}(y_{TM} - z_{TE})\sin\theta\cos\theta\right\} \\ &+ \hat{y}\left\{\frac{\partial E_x}{\partial r}(y_{TM} - z_{TE})\sin\theta\cos\theta\right. \\ &\left. + \frac{\partial E_y}{\partial r}(z_{TE}\cos^2\theta + y_{TM}\sin^2\theta)\right\}\Bigg].\end{aligned} \tag{A6}$$

For the case that $E_x = P_x\tilde{E}_e$ and $E_y = P_y\tilde{E}_o$, (10) is deduced.

REFERENCES

[1] T. Katsuyama and H. Matsumura, *Infrared Optical Fibers*. Bristol, UK and Philadelphia: Adam Hilger, 1989.

[2] M. Miyagi, A. Hongo, and Y. Matsuura, "Hollow IR waveguides," *Soc. Photo-Opt. Instrum. Eng.*, vol. 1228, pp. 26–35, 1990.

[3] M. Miyagi, K. Harada, and S. Kawakami, "Wave propagation and attenuation in the general class of circular hollow waveguides with uniform curvature," *IEEE Trans. Microwave Theory Tech.*, vol. MTT-32, no. 5, pp. 513–531, May 1984.

[4] J. Jiao, W. L. Kath, X. Fang, and M. E. Marhic, "Losses of infrared biconcave metallic whispering-gallery waveguides," *Infrared Phys.*, vol. 29, no. 2–4, pp. 309–321, 1989.

[5] D. Mendlovic, E. Goldenberg, S. Ruschin, J. Dror, and N. Croitoru, "Ray model for transmission of metallic-dielectric hollow bent cylindrical waveguides," *Appl. Opt.*, vol. 28, no. 4, pp. 708–712, Feb. 1989.

[6] S. Abe and M. Miyagi, "Transmission and attenuation of the dominant mode in uniformly bent circular hollow waveguides for the infrared: scalar analysis," *IEEE Trans. Microwave Theory Tech.*, vol. 39, no. 2, pp. 230–238, Feb. 1991.

[7] M. Miyagi and S. Kawakami, "Design theory of dielectric-coated circular metallic waveguides for the infrared transmission," *IEEE J. Lightwave Technol.*, vol. LT-2, no. 2, pp. 116–126, Apr. 1984.

[8] A. W. Snyder and W. R. Young, "Modes of optical waveguides," *J. Opt. Soc. Am.*, vol. 68, no. 3, pp. 297–308, Mar. 1978.

[9] M. Miyagi and S. Kawakami, "Losses and phase constant changes caused by bends in the general class of hollow waveguides for the infrared," *Appl. Opt.*, vol. 20, no. 24, pp. 4221–4226, Dec. 1981.

[10] M. Miyagi and S. Karasawa, "Waveguide losses in sharply bent circular hollow waveguides," *Appl. Opt.*, vol. 29, no. 3, pp. 367–370, Jan. 1990.

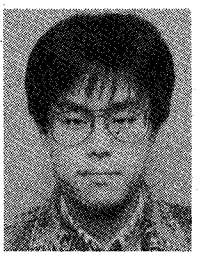

Shin-ichi Abe was born in Yamagata, Japan, on January 12, 1967. He received the B.E. and M.E. degrees from Tohoku University, Sendai, Japan in 1989 and 1991, respectively. He is currently working toward the Ph.D. degree in electrical engineering at Tohoku University. His research interests include optical hollow waveguides.

Mr. Abe is a member of the Institute of Electronics, Information, and Communication Engineers of Japan.

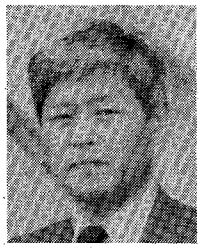

Mitsunobu Miyagi (M'85–SM'90) was born in Hokkaido, Japan, on December 12, 1942. He graduated from Tohoku University, Sendai, Japan in 1965, and received the M.E. and Ph.D. degrees from the same university in 1967 and 1970, respectively.

He was appointed Research Associate at the Research Institute of Electrical Communication, Tohoku University, in 1970. From 1975 to 1977, on leave of absence from Tohoku University, he joined McGill University, Montreal, PQ, Canada, where he was engaged in research on optical communications. In 1978, he became an Associate Professor at the Research Institute of Electrical Communication. Since 1987, he has been a Professor at the Department of Electrical Communications, Faculty of Engineering, Tohoku University. He spent a month at Tianjin University, China, as a Consultant to the International Advisory Panel of the Chinese University Development Project and the Chinese Review Commission of the Chinese Ministry of Education in 1985. His research activities cover fiber optics, integrated optics, and guided wave technology and its application at mid-infrared, especially the design and fabrication of IR waveguides for high-powered CO_2 lasers and waveguide-type lasers. He also has been carrying out some works in electromagnetic theory including nonlinear wave propagation.

Dr. Miyagi is the member of the Institute of Electronics and Communication Engineers of Japan, the Optical Society of America, SPIE, and the American Institute of Physics. In 1989, he was awarded the Ichimura Prize for his contribution to the IR hollow waveguide and its application.